40-Gb/s Optical 3R Regeneration Using a Traveling-wave Electroabsorption Modulator-Based Optical Clock Recovery

Zhaoyang Hu, Hsu-Feng Chou, John E. Bowers and Daniel J. Blumenthal
Department of Electrical & Computer Engineering, University of California, Santa Barbara, CA 93106
Tel: (805) 893-5616, Fax: (805) 893-7990, E-mail:huby@ece.ucsb.edu

Abstract: We demonstrate a novel 40-Gb/s optical 3R regenerator that utilizes a traveling-wave electroabsorption modulator-based optical clock recovery. A regenerative fiber XPM wavelength converter is used to implement re-shaping function. 3R regeneration is demonstrated with a reduced timing jitter.

OCIS codes: (060.2330) Fiber optics communications, (070.4560) Optical data processing

1. Introduction

Optical 3R regeneration (re-amplifying, re-shaping, and re-timing) is a key-function to restore the transmission impairments stemming from fiber chromatic dispersion, fiber nonlinear effects, noise and jitter accumulations in the long-haul optical communication systems. To date, various optical 3R architectures based on fiber, semiconductor optical amplifier (SOA) or electroabsorption modulator (EAM) have been demonstrated [1-4]. In order to re-time and re-shape an optical return-to-zero (RZ) signal, optical clock recovery (OCR) is performed first and the recovered optical clock pulses are launched into a regenerative wavelength converter together with the appropriately delayed optical data signal.

In this paper, we describe a compact optical 3R regenerator using a traveling-wave EAM (TW-EAM)-based OCR [5] combined with a regenerative fiber cross-phase modulation (XPM) wavelength converter [6]. As shown in Fig.1, the TW-EAM-based OCR is injection locked to the clock frequency and imprints the clock tone from the input data signal (λ_1) onto a new wavelength (λ_2). The input data signal is remained or even lateral re-shaped on the original wavelength depending on the width of the synchronized TW-EAM's switch window [7]. The optical recovered clock at λ_2 and the original data at λ_1 from the same output port of the TW-EAM are directly injected into the regenerative wavelength converter for 3R regeneration without any additional timing alignment, which greatly simplifies the regenerator. Furthermore, no additional optical pulse generator is required since it is already imbedded in the TW-EAM-based OCR. The fiber XPM wavelength converter with nonlinear transfer function provides vertical re-shaping function [8] and the converted signal at λ_2 with 3R regeneration is achieved. Compared to the input 40-Gb/s RZ signal, the converted signal has a lower timing jitter due to the spectrum purifying effect of the TW-EAM-based OCR.

2. Principle of 3R Operation

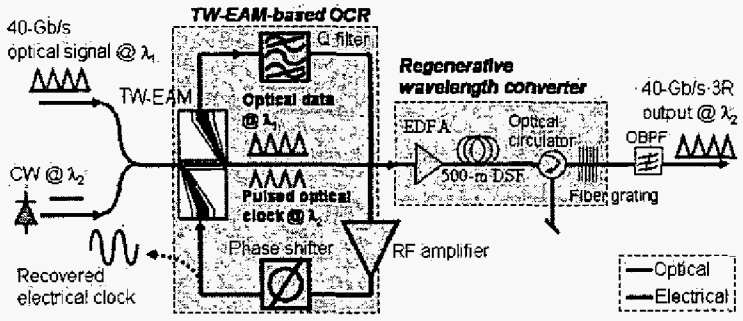

Fig. 1 Optical 3R architecture using a TW-EAM-based OCR (OBPF: optical bandpass filter)

As shown in Fig.1, the TW-EAM-based OCR uses a TW-EAM, an RF Q filter, an RF amplifier and a phase shifter to construct a 40-GHz self-oscillating ring oscillator. If the input optical signal at λ_1 contains a frequency within the OCR's locking range, the OCR can be injection locked. The TW-EAM works simultaneously as a photodetector by using photocurrent from the upper electrical port and a pulsed optical clock generator by applying the recovered

electrical clock on the lower electrical port to modulate the CW light at λ_2. The output signals from the OCR are the 40-Gb/s optical data and the recovered 40-GHz RZ optical clock at separated wavelengths, which are then fed into a subsequent fiber XPM wavelength converter. The wavelength converter is implemented by using XPM in 500-m long dispersion shifted fiber (DSF). 400-mW power level of the input signals is required by the wavelength converter to obtain enough nonlinearity in the DSF fibers. Details of the wavelength converter have been previously reported in [6, 8]. The wavelength converter essentially uses the data as a gate on the recovered clock pulses and finally regenerated 40-Gb/s data at wavelength λ_2 is obtained.

Phase relationship between the optical data and recovered RZ optical clock output from the OCR for subsequent wavelength conversion is critical to 3R performance. In our previous work [5], we have achieved the injection locked oscillation condition for phase is:

$$\phi_1 + \omega_{in}\tau = \phi + 2N\pi \tag{1}$$

where ϕ is the initial phase, ϕ_1 is the resulted phase due to injection locking (i.e., the phase of the recovered electrical and optical clock), ω_{in} is the angular frequency of the injected signal and N is an integer. The injection frequency ω_{in} can be re-written in the form of $\omega_{in} = \omega_{osc} + \Delta\omega$, where ω_{osc} is the free-running frequency of the OCR and $\Delta\omega$ is the offset of ω_{in} to ω_{osc}. Because ω_{osc} satisfies the relation of $\omega_{osc}\tau = 2N\pi$, Eqn. (1) can be rewritten as

$$\phi - \phi_1 = \Delta\omega\tau \tag{2}$$

From Eqn. (2), it is obvious that the recovered optical clock has the same phase as that of the injected signal when the injection frequency is same as the free-running frequency, i.e. $\Delta\omega = 0$. As shown in Fig.2 (a), we observed the phase match of the 40-Gb/s optical signal (upper waveform) and recovered optical clock (lower waveform) from the same output port of the OCR. However, there is a relative phase difference equal to $\Delta\omega\tau$ between the injected signal and recovered optical clock when the injection frequency is different from the free-running frequency, i.e., $\Delta\omega \neq 0$. It is confirmed in Fig.2 (b) when we intentionally change the OCR's free-running frequency 20-kHz offset from the injection frequency but still within the locking range.

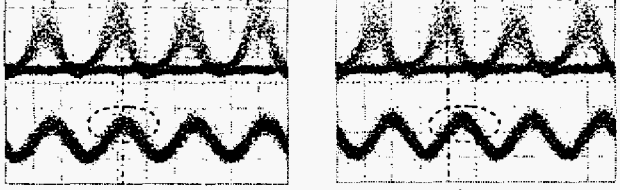

(a) (b)

Fig. 2 (a) Matched phase (b) Mismatched phase of the 40-Gb/s optical signal (upper) and recovered 40-GHz optical clock (lower) from the same output port of OCR

3. Experimental results of 3R wavelength conversion

A 10-GHz gain-switched distributed Bragg reflector (DBR) laser is used to generate pulses at 1552.5 nm (λ_1) and modulated with 2^{31}-1 PRBS pattern by a $LiNbO_3$ modulator and then optically multiplexed to 40-Gb/s optical time division multiplexing (OTDM) signal. The CW light input for generating the recovered optical clock is 3 dBm at 1547.6 nm (λ_2). A 3-dB coupler is used to combine the 40-Gb/s OTDM signal and the CW light together. And then the combined signal is amplified by an EDFA to 12 dBm before entering the OCR. The bias voltage of the TW-EAM is set to 1.06 V considering the output power and modulation efficiency of the TW-EAM. The pulsewidth of the generated optical clock is 10 ps. A shorter pulsewidth can be obtained by increasing the amplitude of the recovered electrical clock applied on the TW-EAM. The locking-range of the OCR is 0.5MHz, within which the relative phase of the optical data and recovered optical clock can be adjusted by the phase shifter to optimize the operation of the subsequent wavelength converter. A fiber XPM wavelength converter with near cosine transfer function is used to imprint the data pattern on the recovered optical clock. The converted 40-Gb/s signal from the wavelength converter is filtered out by a 0.6 nm optical bandpass filter (OBPF).

Fig.3 (a) depicts the optical spectra of output signals from the OCR, the position of optical filter and converted 40-Gb/s signal. Grey line in the Fig.3 (a) shows the output signals from the OCR. CW light at 1547.6 nm is modulated to generate multi-peaks separated at 0.32 nm and it means 40-GHz recovered optical clock. After fiber XPM wavelength converter, the optical spectrum of the recovered optical clock is broadened and one of its sidebands is filtered out as the converted 40-Gb/s signal. The position of the optical filter is shown as the dashed line in the Fig.3 (a).

The single sideband (SSB) noise spectra of the input 40-Gb/s OTDM signal, recovered optical clock and converted 40-Gb/s signal (with EDFA amplification) are obtained by connecting directly to an RF spectrum analyzer via a 50-GHz bandwidth photodiode, which are shown as light dark line, heavy dark line and grey line in Fig.3 (b), respectively. Through integrating the noise spectra from offset frequency of 1 kHz to 10 MHz, the root-mean-square timing jitters for the input signal, recovered clock and converted signal are 871 fs, 425 fs and 537 fs, respectively.

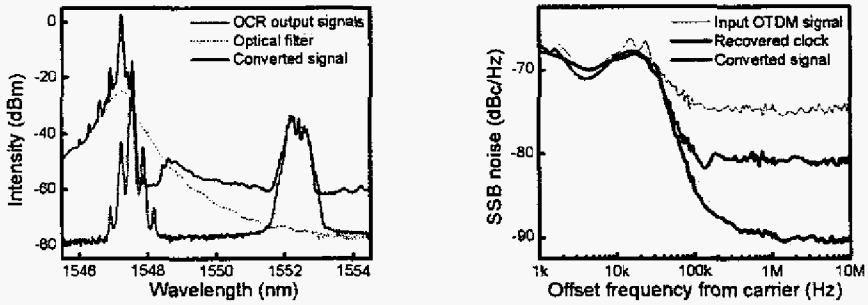

Fig. 3 (a) Optical spectra of output signals from the OCR, optical filter and wavelength converted signal (b) SSB noise spectra of input signal, recovered clock, and wavelength converted signal (Resolution bandwidth: 200Hz)

Fig.4 shows the BER curves and the eye diagrams of the 40-Gb/s back-to-back and 3R wavelength converted signals. The inset waveforms in Fig. 4 show the corresponding eye diagrams. Compared with the back-to-back results, the average power penalty is 2.7 dB. The power penalties were mainly caused by the relatively low power level -10 dBm of the OCR's output signals to the fiber XPM wavelength converter since the TW-EAM introduces 20-dB insertion loss mainly from coupling loss. Reducing the TW-EAM's loss and using a relative low input power wavelength converter can improve the 3R performance.

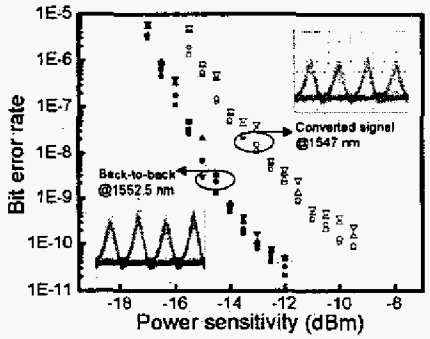

Fig. 4 BER curves and eye diagrams of the 40-Gb/s OTDM input signal and 3R wavelength converted signal

4. Summary and Conclusion

A compact 40-Gb/s optical 3R regeneration using a TW-EAM-based OCR is proposed and demonstrated. The signals from the same output port of the OCR, i.e., the data signal and recovered optical clock, are directly injected into a wavelength converter for 3R regeneration without any additional timing adjustment or optical pulse generator. 3R wavelength conversion results show 40% timing jitter reduction. Further 3R performance could be improved by reducing the TW-EAM's loss. The authors would like to acknowledge funding for this project under KDDI under grant 442530-59406 and a State of California UC Discovery grant 597095-19929.

References

[1] O. Leclerc, et al., J. Lightwave. Technol., vol. 21, pp. 2779-2790, Nov. 2003.
[2] T. Otani, T. Miyazaki, and S. Yamamoto, J. Lightwave Technol., Vol. 20, pp. 195-200, 2002.
[3] E. S. Awad, et al., IEEE Photon. Technol. Lett., vol. 14, pp. 1378-1380, Sep. 2002.
[4] K. Nishimura, et al., pp. 286-287, ECOC2001.
[5] Z. Hu, et al., IEEE Photon. Technol. Lett., vol. 16, pp. 1376-1378, 2004.
[6] B.-E. Olsson, et al., IEEE Photon. Technol. Lett., vol. 12, pp. 846-848, 2000.
[7] Z. Hu, et al., Paper We 3.5.4, ECOC2004.
[8] P. Ohlen, et al., IEEE Photon. Technol. Lett., vol. 12, pp. 522-524, 2000.